Atmospheric Environment 152 (2017) 477–489

Contents lists available at ScienceDirect

Atmospheric Environment

journal homepage: www.elsevier.com/locate/atmosenv

# Point-surface fusion of station measurements and satellite observations for mapping $PM_{2.5}$ distribution in China: Methods and assessment

Tongwen Li [a], Huanfeng Shen [a, b, c, *], Chao Zeng [d], Qiangqiang Yuan [e], Liangpei Zhang [b, f]

[a] School of Resource and Environmental Sciences, Wuhan University, Wuhan, Hubei 430079, China
[b] The Collaborative Innovation Center for Geospatial Technology, Wuhan, Hubei 430079, China
[c] The Key Laboratory of Geographic Information System, Ministry of Education, Wuhan University, Wuhan, Hubei 430079, China
[d] The State Key Laboratory of Hydroscience and Engineering, Department of Hydraulic Engineering, Tsinghua University, Beijing 100084, China
[e] School of Geodesy and Geomatics, Wuhan University, Wuhan, Hubei 430079, China
[f] The State Key Laboratory of Information Engineering in Surveying, Mapping and Remote Sensing, Wuhan University, Wuhan, Hubei 430079, China

## HIGHLIGHTS

- A national-scale GRNN model is developed to estimate $PM_{2.5}$ concentration in China.
- The performance of the widely used models is comprehensively evaluated and compared.
- A pixel-based merging strategy is proposed to map the mean $PM_{2.5}$ distribution.

## ARTICLE INFO

*Article history:*
Received 24 June 2016
Received in revised form
23 December 2016
Accepted 2 January 2017
Available online 3 January 2017

*Keywords:*
Satellite remote sensing
Point-surface fusion
AOD
$PM_{2.5}$
GRNN
Assessment

## ABSTRACT

Fine particulate matter ($PM_{2.5}$, particulate matters with aerodynamic diameters less than 2.5$\mu m$) is associated with adverse human health effects, and China is currently suffering from serious $PM_{2.5}$ pollution. To obtain spatially continuous ground-level $PM_{2.5}$ concentrations, several models established by the point-surface fusion of station measurements and satellite observations have been developed. However, how well do these models perform at national scale in China? Is there space to improve the estimation accuracy of $PM_{2.5}$ concentration? The contribution of this study is threefold. Firstly, taking advantage of the newly established national monitoring network, we develop a national-scale generalized regression neural network (GRNN) model to estimate $PM_{2.5}$ concentrations. Secondly, different assessment experiments are undertaken in time and space, to comprehensively evaluate and compare the performance of the widely used models. Finally, to map the yearly and seasonal mean distribution of $PM_{2.5}$ concentrations in China, a pixel-based merging strategy is proposed. The results indicate that the conventional models (linear regression, multiple linear regression, and semi-empirical model) do not obtain the expected results at national scale, with cross-validation R values of 0.49–0.55 and RMSEs of 30.80–31.51$\mu g/m^3$, respectively. In contrast, the more advanced models (geographically weighted regression, back-propagation neural network, and GRNN) have great advantages in $PM_{2.5}$ estimation, with R values ranging from 0.61 to 0.82 and RMSEs from 20.93 to 28.68$\mu g/m^3$, respectively. In particular, the proposed GRNN model obtains the best performance. Furthermore, the mapped $PM_{2.5}$ distribution retrieved from 3-km MODIS aerosol optical depth (AOD) products agrees quite well with the station measurements. The results also show that the approach used in this study has the capacity to provide reasonable information for the global monitoring of $PM_{2.5}$ pollution in China.



## 1. Introduction

Fine particulate matter ($PM_{2.5}$, particulate matters with aerodynamic diameters less than 2.5$\mu m$) can carry toxic and harmful

* Corresponding author. School of Resource and Environmental Sciences, Wuhan University, Wuhan, Hubei 430079, China
*E-mail addresses:* litw@whu.edu.cn (T. Li), shenhf@whu.edu.cn (H. Shen), zengchaozc@hotmail.com (C. Zeng), yqiang86@gmail.com (Q. Yuan), zlp62@whu.edu.cn (L. Zhang).

http://dx.doi.org/10.1016/j.atmosenv.2017.01.004
1352-2310/

substances and travel across countries and geographic boundaries (Engel-Cox et al., 2013). Many epidemiological studies have shown that long-term exposure to $PM_{2.5}$ is associated with adverse health effects (Bartell et al., 2013; Sacks et al., 2011). With the rapid economic development, China is suffering from serious air pollution, and $PM_{2.5}$ has gradually become the primary pollutant, which has attracted widespread social concern (Peng et al., 2016; Yuan et al., 2012). Consequently, $PM_{2.5}$ has been incorporated into the new air quality standard of the Chinese government (GB 3095-2012). Since January 2013, hourly $PM_{2.5}$ concentrations have been disclosed to the public through the China National Environmental Monitoring Center (CNEMC) website (http://www.cnemc.cn). By the end of 2014, about 1500 monitoring sites had been established to report the overall air quality in China.

Despite the high precision and stability (Fang et al., 2016; Lin et al., 2015), there are still some limitations to the spatiotemporal analysis due to the sparse and uneven distribution of the ground stations. Unlike the ground-level measurements, satellite-based observation has the capacity to provide wide-coverage data. Using both the ground station measurements and co-located satellite observations, the relationship between the various observed variables can be established. Based on this relationship and its variation rule in space, spatially continuous data can be reconstructed. This method, which can generate data from point scale to surface scale, is known as “point-surface fusion”. The point-surface fusion of station-level $PM_{2.5}$ measurements and satellite-based aerosol optical depth (AOD, also called aerosol optical thickness) can obtain spatially continuous $PM_{2.5}$ data, and has the potential to compensate for the spatiotemporal limitation. Several widely used models, established by point-surface fusion, have been developed to describe the relationship between PM and AOD (AOD-PM relationship) (Beloconi et al., 2016; Chu et al., 2003; Hoff and Christopher, 2009; Kloog et al., 2014; Li et al., 2005, 2011; Liu et al., 2007; Martin, 2008).

According to a previous study (Lin et al., 2015), the existing models, which were developed to retrieve ground-level $PM_{2.5}$ concentrations using satellite observations, can be classified into two main categories: simulation-based models and observation-based models. Simulation-based models (Geng et al., 2015; Liu et al., 2004; van Donkelaar et al., 2010) consider the effects of both meteorology and aerosol properties, which are simulated with global or regional chemical transport models. These models would be most suitable for predicting $PM_{2.5}$ concentration if we have comprehensive datasets (especially emission inventories) and a good understanding of the $PM_{2.5}$ formation and removal processes. Given the complexity of the problem, an observation-based model is a good compromise (Gupta and Christopher, 2009a). Observation-based models rely on the statistical relationship between AOD and in situ $PM_{2.5}$ measurements, and are much easier to implement, but with an almost equivalent accuracy of $PM_{2.5}$ estimation to the simulation-based models. Hence, the observation-based models, established by point-surface fusion, have been extensively discussed and studied. Using a simple linear regression model between AOD and $PM_{2.5}$, early studies obtained some reasonable results (Chu et al., 2003; Wang et al., 2010). However, the relationship tends to be influenced by region and time due to the effects of variations in emissions and meteorological conditions. Through incorporating more meteorological parameters (e.g., relative humidity, temperature, wind speed), a multiple linear regression model may better represent the AOD-$PM_{2.5}$ relationship (Benas et al., 2013; Gupta and Christopher, 2009b). Unlike the empirical models, semi-empirical models take the related physical understanding into account (Liu et al., 2005; Tian and Chen, 2010; You et al., 2015), and attempt to introduce physical prior knowledge to solve the problem. More recently, allowing for the spatial heterogeneity of the AOD-$PM_{2.5}$ relationship, a more advanced statistical model called geographically weighted regression (GWR) has been developed to estimate $PM_{2.5}$ concentration (Hu et al., 2013; Song et al., 2014; You et al., 2015). This model predicts $PM_{2.5}$ concentration using a local regression approach instead of globally constant regression parameters. In addition, as one of the intelligent algorithms, artificial neural networks (ANNs) have the potential to better represent the complex nonlinear relationship. Hence, ANNs have been introduced into the estimation of $PM_{2.5}$ concentration (Gupta and Christopher, 2009a; Wu et al., 2012; Yao and Lu, 2014), which has been gradually considered to be a multivariable and nonlinear problem. Furthermore, some more complex mixed effects models and generalized additive mixed (GAM) models have been developed (Kloog et al., 2011; Liu et al., 2009). On the other hand, considering the effect of the main aerosol characteristics, an observation-based method was developed by establishing a multi-parameter remote sensing formula of $PM_{2.5}$ concentration (Li et al., 2016; Lin et al., 2015; Zhang and Li, 2015). All these observation-based models have been widely used, and have played an irreplaceable role in satellite-based estimation of $PM_{2.5}$ concentration.

China is now facing a serious $PM_{2.5}$ pollution problem (Peng et al., 2016; Zhang and Cao, 2015). Because of the wide geographical range and complex terrain, mapping the distribution of $PM_{2.5}$ concentration in China is faced with lots of challenges. To date, many researchers have made attempts to study the AOD-PM relationship in China (Guo et al., 2009; Li et al., 2005, 2011; Lin et al., 2015; Song et al., 2014; Wang et al., 2010; Wu et al., 2012). Due to the unavailability of sufficient $PM_{2.5}$ measurements in China before 2013, most of the studies have used a limited number of ground-level $PM_{2.5}$ measurements at regional scale. However, the regional estimation and analysis of $PM_{2.5}$ concentration cannot provide sufficient information for the macroscopical monitoring of the whole of China. With the newly available national $PM_{2.5}$ measurements since January 2013, a few attempts (Lin et al., 2015; Ma et al., 2014, 2016) have been made to estimate $PM_{2.5}$ concentration at national scale. However, the methods and data used in these studies to establish the AOD-$PM_{2.5}$ relationship differ greatly from one another. Additionally, the validation schemes of the models have many differences; for instance, some schemes undertook validation based on yearly/monthly averages, and some on a daily basis. Thus, the intercomparison of national-scale model performance is not possible. Furthermore, previous studies (Hoff and Christopher, 2009) have suggested that the models may perform differently in different regions. As a result, when we focus on the national studies, the performance of the models developed in regional studies still needs to be evaluated and compared. On the other hand, although the widely used models have achieved reasonable results under certain conditions, the estimation accuracy of $PM_{2.5}$ concentration still has room for improvement (De Leeuw et al., 2006; Song et al., 2014).

In this paper, one of the main objectives is to develop an advanced model (generalized regression neural network, GRNN) which can better represent the AOD-$PM_{2.5}$ relationship for the prediction of $PM_{2.5}$ distribution in China. Another main objective is to comprehensively evaluate and analyze the performance of the widely used models at national scale. Finally, a direct average only reflects the level of $PM_{2.5}$ pollution on those days with valid AOD data, so a pixel-based merging strategy is proposed to map the yearly and seasonal mean distribution of $PM_{2.5}$ concentrations.

## 2. Data and measurements

### 2.1. Ground-level $PM_{2.5}$ measurements

Daily average $PM_{2.5}$ concentration data from February 2013 to December 2014 were obtained from the China National Environmental Monitoring Center (CNEMC) website (http://www.cnemc.cn). The monitoring network is being continuously updated, and the number of monitoring sites has increased from ~500 in early 2013 to ~1500 by the end of 2014. According to the Chinese National Ambient Air Quality Standard (CNAAQS, GB3905-2012), the ground-level $PM_{2.5}$ concentration should be measured by the tapered element oscillating microbalance method (TEOM) or with beta attenuation monitors (BAMs or beta-gauge), with an uncertainty of 0.75% for the hourly record (Engel-Cox et al., 2013). Fig. 1 shows the spatial distribution of the $PM_{2.5}$ monitoring sites in China.

### 2.2. MODIS AOD products

The Moderate Resolution Imaging Spectroradiometer (MODIS) onboard the Earth Observing System (EOS) satellites, Terra and Aqua, can provide retrieval products of aerosol and cloud properties with a nearly daily global coverage (Remer et al., 2005). Recently, a new version (Collection 6) of the MODIS aerosol products has been released at a higher spatial resolution (3 km at nadir). Both the newly released 3-km products and the prior standard 10-km AOD products are retrieved using the dark target algorithm, whereas a single retrieval box of 6 × 6 pixels and 20 × 20 pixels is averaged, respectively. Moreover, the pixels outside the reflectivity range of the brightest 50% and darkest 20% at 0.66$\mu m$ are discarded to reduce the uncertainty for the 3-km AOD products (Munchak et al., 2013).

Both MODIS Terra and Aqua 3-km AOD products corresponding to the ground $PM_{2.5}$ measurements were downloaded from the Level 1 and Atmosphere Archive and Distribution System (LAADS) website (http://ladsweb.nascom.nasa.gov). The coverage of these two AOD products differs because of the different crossing times of the two sensors. Hence, linear regression analysis is conducted between those pixels where both AOD products are present for each day, and the regression coefficients are used to predict the missing Aqua AOD values from the corresponding available Terra AOD, and vice versa (Hu et al., 2014b). The average of the two AOD products is then used to estimate $PM_{2.5}$ concentrations.

### 2.3. Meteorological data

The National Aeronautics and Space Administration (NASA) atmospheric reanalysis data known as the second Modern-Era Retrospective Analysis for Research and Applications (MERRA-2) (Molod et al., 2015) data were used in this study. These data are generated using the Goddard Earth Observing System Model Version 5 (GEOS-5) data assimilation system, which is able to assimilate the newer microwave sounders and hyperspectral infrared radiance instruments, as well as other data types. The MERRA-2 meteorological data are available from 1980, with a

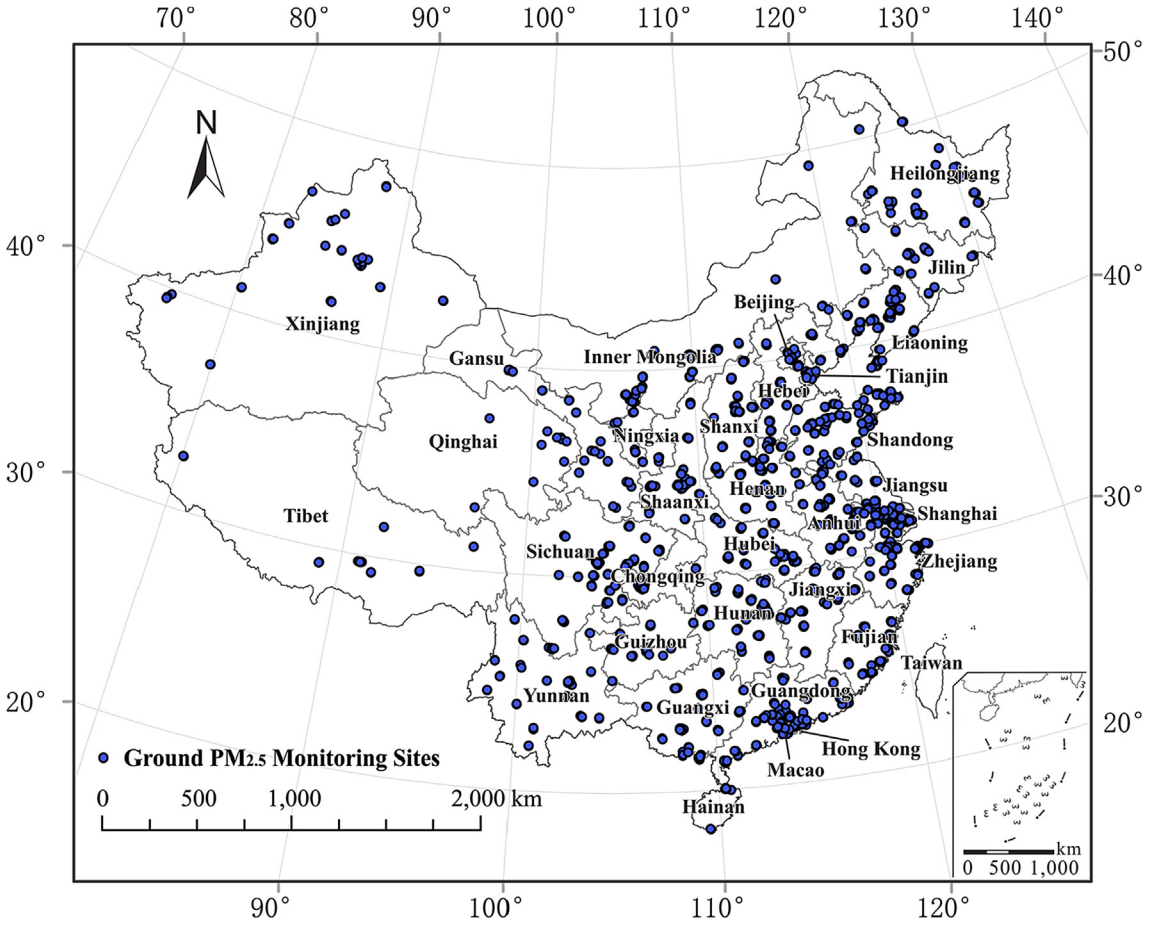


**Fig. 1.** Spatial distribution of $PM_{2.5}$ monitoring sites in China, as of the end of 2014.

spatial resolution of 0.625° longitude × 0.5° latitude. More details can be found at the website (http://gmao.gsfc.nasa.gov/GMAO_products/).

We extracted relative humidity (RH, %), air temperature at a 2 m height (TEMP, K), wind speed at 10 m above ground (WS, m/s), surface pressure (SP, Pa), and planetary boundary layer height (HPBL, m) between 10 a.m. and 11 a.m. local time (the Terra satellite overpass time corresponds to 10:30 a.m. local time), and 1 p.m. and 2 p.m. local time (the Aqua satellite overpass time corresponds to 1:30 p.m. local time), respectively. Each parameter was averaged over the two periods to supplement the predictors for the estimation of $PM_{2.5}$ concentrations.

### 2.4. Data preprocessing and matching

All the above data were reprocessed to be consistent temporally and spatially to form a complete dataset which could serve as the foundational samples for the model development. Firstly, the satellite AOD and meteorological reanalysis data were regridded to 0.03°. Secondly, all the data were reprojected to the same projection coordinate system. Finally, ground $PM_{2.5}$ measurements were associated with the value of the satellite AOD and meteorological data covering the station. The averaging over multiple pixels is expected to effectively reduce random errors, but the best size of a single window centered at a given $PM_{2.5}$ monitoring station still remains unclear for our analysis. Hence, three different window sizes of 1 × 1, 3 × 3, 5 × 5 pixels were applied, respectively. The results show that the averaging scheme over a window size of 3 × 3 pixels reported a slight advantage, which is consistent with previous studies (Wu et al., 2012; You et al., 2015). After the data preprocessing and matching, a total of 77,978 records from the multi-source data (spanning almost 2 years and containing ground-level $PM_{2.5,}$ satellite-derived AOD, and MERRA meteorological data) were collected for the model development.

## 3. Methodology

### 3.1. Previous retrieval models

#### 3.1.1. Corrected linear regression (CLR)

The linear regression model was used in earlier studies (Chu et al., 2003). However, later studies reported better performances after meteorological correction (Li et al., 2005; Wang et al., 2010). Hence, the CLR model was used in this study:

$$PM'_{2.5} = a + b \cdot \frac{AOD}{HPBL} \tag{1}$$

$$PM'_{2.5} = PM_{2.5} \cdot \left(\frac{1}{1 - RH/100}\right) \tag{2}$$

where AOD is the aerosol optical depth, and $PM'_{2.5}$ denotes the RH-corrected $PM_{2.5.}$

#### 3.1.2. Multiple linear regression (MLR)

Through incorporating more meteorological parameters, MLR has been introduced into the prediction of $PM_{2.5}$ concentration (Benas et al., 2013; Gupta and Christopher, 2009b). Based on empirical statistics, it can be defined as:

$$PM_{2.5} = \beta_0 + \beta_1 \cdot AOD + \beta_2 \cdot TEMP + \beta_3 \cdot RH + \beta_4 \cdot WS + \beta_5 \cdot HPBL + \beta_6 \cdot SP \tag{3}$$

where $\beta_0$ is the interception for $PM_{2.5}$ prediction, and $\beta_1 \sim \beta_6$ are regression coefficients for the predictor variables.

#### 3.1.3. Semi-empirical model (SEM)

Based on related physical understanding and statistical theory, SEM was developed to describe the relationship between meteorological data, AOD, and $PM_{2.5}$ (Liu et al., 2005; Tian and Chen, 2010). It can be expressed as:

$$PM_{2.5} = e^{\beta_0 + \beta_2 \cdot TEMP + \beta_3 \cdot RH} \cdot AOD^{\beta_1} \cdot WS^{\beta_4} \cdot HPBL^{\beta_5} \tag{4}$$

#### 3.1.4. Geographically weighted regression (GWR)

The GWR model was developed to account for the spatial heterogeneity of the AOD-$PM_{2.5}$ relationship (Hu et al., 2013; You et al., 2015). The GWR model does not predict $PM_{2.5}$ concentration using globally constant parameters, but generates continuous parameters by local model fitting. It can be represented as Eq. (5):

$$PM_{2.5,i} = \beta_{0,i} + \beta_{1.i} \cdot AOD + \beta_{2,i} \cdot TEMP + \beta_{3,i} \cdot RH + \beta_{4,i} \cdot WS + \beta_{5,i} \cdot HPBL + \beta_{6,i} \cdot SP \tag{5}$$

where the meanings of the variables and coefficients are the same as Eq. (3), but based on local regression over station *i*, and hence the coefficients vary in space. In this study, the adaptive bandwidths were used because of the uneven distribution of the $PM_{2.5}$ stations.

#### 3.1.5. Back-propagation neural network (BPNN)

With more and more predictors, the estimation of $PM_{2.5}$ concentration has been gradually considered to be a multi-variable and nonlinear problem. Consequently, ANNs, which have the potential to extract trends in imprecise and complicated nonlinear data (Gupta and Christopher, 2009a), have been introduced into $PM_{2.5}$ estimation (Wu et al., 2012; Yao and Lu, 2014). The most common training algorithm is back-propagation (BP). A BPNN model with three layers (input layer, hidden layer, and output layer) was constructed in our study. The input parameters were latitude, longitude, month, AOD, TEMP, RH, WS, HPBL, and SP. According to previous studies (Gardner and Dorling, 1998; Reich et al., 1999), the number of nodes in the hidden layer ranges from $2\sqrt{n} + \mu$ to $2n + 1$, where $n$ and $\mu$ are the number of nodes in the input layer and output layer, respectively. Thus, the number of nodes in the hidden layer was varied from 7 to 19, and 18 nodes (which performed the best) were selected in this paper.

### 3.2. Proposed generalized regression neural network (GRNN) model

Previous studies (Gupta and Christopher, 2009a; Ordieres et al., 2005) have indicated that ANNs can outperform the classic statistical models. However, the well-known BPNN has the disadvantages of slow convergence and easily converging to a local minimum (Yu, 1992). Hence, we apply here another neural network named the GRNN, which can overcome the shortcomings of the BPNN (Cigizoglu and Alp, 2006). The GRNN is often used for function approximation, and it can be considered as a normalized radial basis function (RBF) network. Unlike the BPNN, the hidden nodes of the GRNN are often connected by a Gaussian function, which is locally distributed and attenuated to the center of the radial symmetry. This results in local approximation ability and rapid learning velocity. Additionally, the GRNN has few parameters that need to be artificially set in advance, so it can learn the potential relationship between variables up to the hilt. A common GRNN architecture has

three layers of neurons: the input layer, the RBF hidden layer, and the special linear output layer. The input layer and RBF hidden layer are usually connected by a density function. The output of the hidden layer is not directly connected to the output layer by a linear function, but is first connected by a transition of a dot function, reflecting the specialty of the output layer. Further theoretical details can be found in previous studies (Specht, 1991, 1993).

In our study, the input signals are latitude, longitude, month, AOD, TEMP, RH, WS, HPBL, and SP, and the output parameter is $PM_{2.5}$ concentration. The main function of the GRNN model is to estimate a nonlinear regression surface of $PM_{2.5}$ from these input signals. The GRNN model here predicts $PM_{2.5}$ concentration using AOD and meteorological parameters, which are primary and supplementary predictors, respectively. In particular, allowing for the temporal and spatial variation of the AOD-$PM_{2.5}$ relationship, the latitude, longitude, and month are also input to better estimate $PM_{2.5}$ concentration. Unlike the BPNN, the number of nodes in the hidden layer of the GRNN is obtained from training without artificial intervention. The schematics of the GRNN used to estimate $PM_{2.5}$ are presented in Fig. 2.

### 3.3. Model evaluation

The 10-fold cross-validation technique (Rodriguez et al., 2010) was applied to test the model overfitting and predictive power. The dataset was averagely divided into 10 folds randomly. Nine folds of the dataset were used for model fitting, and one fold was predicted in each round of the cross-validation. This step was repeated 10 times until every fold was tested. Statistical indicators, including the correlation coefficient (R), root-mean-square error (RMSE, $\mu g/m^3$), mean prediction error (MPE, $\mu g/m^3$), and relative prediction error (RPE, defined as RMSE divided by mean ground $PM_{2.5}$), were adopted to evaluate the performance of the models.

### 3.4. Mapping strategy for the mean $PM_{2.5}$ distribution

The 3-km MODIS AOD products share a generic feature with prior standard AOD products, which is the absence of data due to clouds or high surface reflectance. Due to the absence of AOD data, the temporally continuous $PM_{2.5}$ data cannot be retrieved at the same location. When we map the temporal mean distribution of $PM_{2.5}$, a direct average can only reflect the level of $PM_{2.5}$ pollution on certain days. To address this issue, a pixel-based merging strategy is proposed, referring to the related studies of spatiotemporal fusion (Shen et al., 2013; Wu et al., 2013, 2015). Firstly, a spatial $PM_{2.5}$ map on every day can be interpolated by station measurements. Due to the sparse distribution of the stations, this map is relatively coarse in space, but still keeps the temporal trend. Thus, the variation of the interpolated $PM_{2.5}$ remains equal to that of the satellite-derived $PM_{2.5}$ at the same location during the same period, and can be represented as Eq. (6):

$$L_{i,p} - L_{i,m} = F_{i,p} - F_{i,m} + \varepsilon_{i,m,p} \quad (6)$$

where $L_{i,m}$ denotes the $PM_{2.5}$ at pixel $i$ on day $m$ interpolated by station measurements using the inverse distance weighting (IDW) approach, and $F_{i,m}$ is the satellite-based estimation of $PM_{2.5}$ at pixel $i$ on day $m$, as are $L_{i,p}$ and $F_{i,p}$. $\varepsilon_{i,m,p}$ is the random error, which will be reduced or eliminated by temporal averaging. For pixel $i$, assuming that $F_{i,p}$ is missing and needs to be estimated, then $m$ is the closest day with valid $PM_{2.5}$ data at the same location to day $p$. Thus, the missing satellite-derived $PM_{2.5}$ data can be reconstructed, and we can map the mean distribution of $PM_{2.5}$ concentration in China.

Some previous studies (van Donkelaar et al., 2012; Zheng et al., 2016) used annual/seasonal mean surface $PM_{2.5}$ measurements to correct this potential sampling bias. They calculated correction factors for each monitoring station/grid, and then the factors were extrapolated to the entire study region. By applying the correction

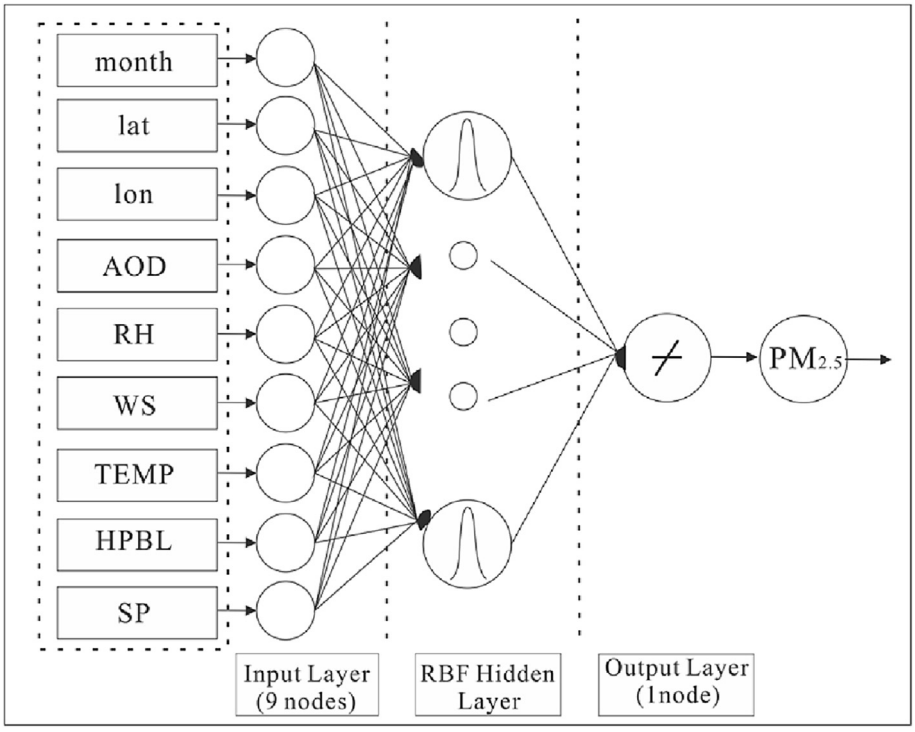


**Fig. 2.** Schematic of the GRNN used to estimate $PM_{2.5}$ concentration in China.

factors for each pixel/grid to predict annual/seasonal average $PM_{2.5}$, the bias-corrected $PM_{2.5}$ concentration can be obtained. Hence, our mapping strategy is compared with this bias-correction method (we denote this as "BCM").

## 4. Results and discussion

### 4.1. Assessment of the various models

#### 4.1.1. Performance of the models

Table 1 shows the performance of the various models. In model fitting, R values range from 0.49 to 0.89, and RMSEs from 16.51 to 31.64$\mu g/m^3$. In the cross-validation results, a similar trend appears. Using simple linear regression, the CLR model performs the worst, with an R value of 0.49 for the cross-validation. There is a large improvement (0.49–0.53 for R) from the CLR model to the MLR model, which considers more meteorological factors. Through introducing some physical prior knowledge, the SEM model shows an advantage in $PM_{2.5}$ estimation, with an R value of 0.55 and an RMSE of 30.80$\mu g/m^3$. Unlike the above models, the GWR model incorporates spatial information into the AOD-$PM_{2.5}$ relationship, and shows a large improvement over the SEM model, with R increasing by 0.06 and RMSE decreasing by 2.12$\mu g/m^3$, respectively. As one of the intelligent algorithms, the BPNN model has the capacity to better represent the AOD-$PM_{2.5}$ relationship, with R and RMSE values of 0.69 and 25.96$\mu g/m^3$, respectively. Compared with the results of the BPNN model, R increases by 0.13 (from 0.69 to 0.82) and RMSE decreases by 5.03$\mu g/m^3$(from 25.96 to 20.93$\mu g/m^3$) for the cross-validation of the GRNN model. These findings suggest that the proposed GRNN model performs the best, followed by BPNN and GWR, and then SEM and MLR, whereas the CLR model obtains the worst performance at national scale.

Furthermore, it should be noted that the conventional models (CLR, MLR, and SEM) have all obtained reasonable results at regional scale in China (Li et al., 2005; Song et al., 2014; Wang et al., 2010), but they do not obtain the expected performance at national scale, with R values of 0.49–0.55 and RMSEs of 30.80–31.51$\mu g/m^3$ for the cross-validation. The results indicate that the conventional models cannot adequately represent the association between $PM_{2.5}$ and independent variables at national scale. However, with R values ranging from 0.61 to 0.82 and RMSEs from 20.93 to 28.68$\mu g/m^3$, the more advanced models (GWR, BPNN, and GRNN) show a great advantage in the estimation of $PM_{2.5}$ concentration.

Allowing for the superiority of the GRNN model, we further evaluated and analyzed its performance. Fig. 3 shows the scatter plots for the GRNN model fitting and cross-validation. From the model fitting to cross-validation, R decreases by 0.07 (from 0.89 to 0.82). The results demonstrate that the proposed model results in slight overfitting (Hu et al., 2014a). However, with the highest cross-validation R (shown in Table 1), the proposed GRNN model outperforms the other models. Therefore, despite the slight overfitting, the GRNN model is more effective for the estimation of $PM_{2.5}$ concentration in China. The cross-validation RPE value is 35.09%, which is almost the same level as a previous national study (Ma et al., 2016). However, a relatively small slope of less than one is reported, indicating some evidence for bias. The possible reason for this is that our model tends to underestimate when ground $PM_{2.5}$ is high. In addition, China has a relatively high level of $PM_{2.5}$, resulting in an intercept that is much greater than zero. Similar results were also found in previous studies (Gupta and Christopher, 2009a; Ma et al., 2014). There is a concern over whether these models can enable epidemiologists to estimate the adverse effects of $PM_{2.5}$ at high levels of $PM_{2.5}$.

**Table 1**
Performance of the various models.

| | Model fitting (N = 70,180) | | | | Cross-validation (N = 77,978) | | | |
|---|---|---|---|---|---|---|---|---|
| | R | RMSE | MPE | RPE | R | RMSE | MPE | RPE |
| CLR | 0.49 | 31.64 | 23.15 | 52.86% | 0.49 | 31.51 | 23.15 | 52.83% |
| MLR | 0.53 | 30.52 | 21.92 | 51.18% | 0.53 | 30.52 | 21.92 | 51.17% |
| SEM | 0.55 | 30.78 | 21.28 | 51.69% | 0.55 | 30.80 | 21.25 | 51.63% |
| GWR | 0.62 | 28.23 | 19.98 | 47.12% | 0.61 | 28.68 | 20.51 | 48.57% |
| BPNN | 0.70 | 25.90 | 18.03 | 43.38% | 0.69 | 25.96 | 18.06 | 43.35% |
| GRNN | 0.89 | 16.51 | 11.01 | 27.66% | 0.82 | 20.93 | 13.90 | 35.09% |

To further analyze the spatial performance of the GRNN model, the R and RMSE values between the observed and estimated $PM_{2.5}$ over the stations were calculated and are presented in Fig. 4. The correlation coefficients at 727 out of 828 stations are greater than 0.80, and 84.90% of the total stations report a low RMSE of less than 20.00$\mu g/m^3$. Spatially, the higher R values are clustered in Eastern China, indicating the accurate estimation of $PM_{2.5}$ concentration in this area. In contrast, the lower R values are found in Northwest China, which is probably caused by the sparse distribution of the ground stations in this area. Moreover, a higher RMSE cluster appears in the Beijing-Tianjin-Hebei (BTH) region and its surroundings. However, it should be noted that the level of $PM_{2.5}$ concentration in the BTH region is relatively high (Lin et al., 2015).

#### 4.1.2. Seasonal variation of model performance

Previous studies have shown that the models can perform differently as a function of the seasons (Gupta and Christopher, 2009a; Lin et al., 2015). Therefore, all the models were respectively established in each season to investigate and compare the seasonal variation of model performance. The seasons were defined as spring (March–May), summer (June–August), autumn (September–November), and winter (December–February), for which the numbers of data records were 21,573, 23,244, 26,281, and 6880, respectively. Fig. 5 shows the seasonal variation of model performance for the cross-validation.

As shown in Fig. 5, the GRNN model performs the best in every season (R = 0.82, 0.82, 0.83, and 0.84 for the cross-validation in spring, summer, autumn, and winter, respectively), followed by BPNN and GWR, and then MLR and SEM, and the simple CLR model obtains the poorest performance (the R values of the four seasons are 0.35, 0.59, 0.57, and 0.50, respectively). The results demonstrate that by taking more meteorological parameters into consideration, the relatively advanced models can significantly improve the accuracy of $PM_{2.5}$ estimation. Furthermore, for each season, the GWR model performs a little worse than the BPNN, but better than the conventional models, indicating that incorporating spatial information into the statistical model can better describe the AOD-$PM_{2.5}$ relationship. Among the four seasons, all the models achieve the poorest performance in spring, which is probably caused by the influence of the enhanced contribution of dust particles (Zhang and Cao, 2015).

On the other hand, all the models generally perform better at seasonal scale (except for spring) than yearly scale, reflecting the influence of the seasons on the AOD-$PM_{2.5}$ relationship. It should be noted that the conventional models (CLR, MLR, and SEM) report a more significant improvement of R value from yearly scale to seasonal scale, indicating that they seem to be more suitable for seasonal observation than yearly observation.

#### 4.1.3. Geographical variation of model performance

Geographical location is considered to be one of the factors which has an influence on the AOD-$PM_{2.5}$ relationship (Hoff and Christopher, 2009). To explore the geographical variation of model performance, all the models were respectively established in every 4° × 4° grid box, as in the study of Gupta and Christopher

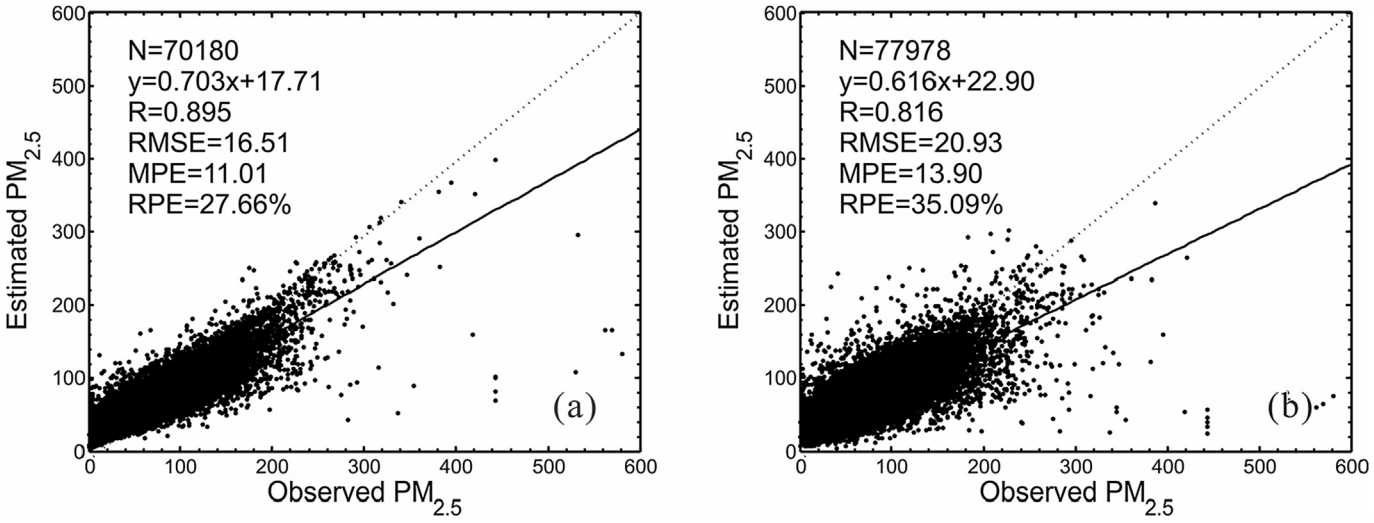


**Fig. 3.** Results of GRNN (a) model fitting and (b) cross-validation. $PM_{2.5}$ unit:$\mu g/m^3$. The dashed line is the 1:1 line.

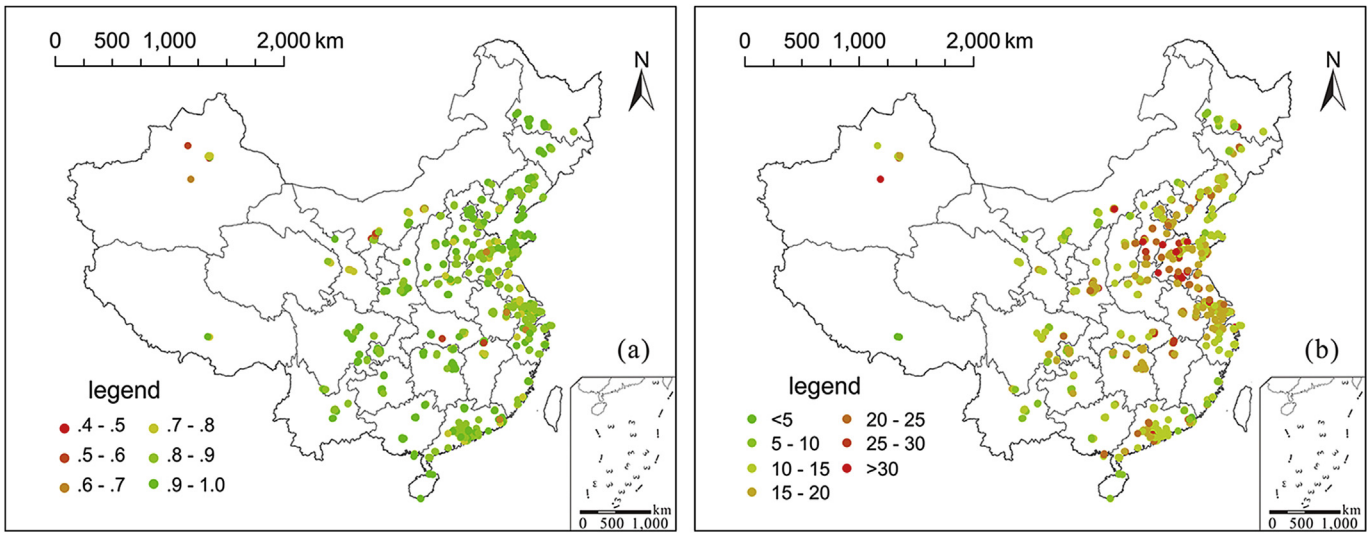


**Fig. 4.** Spatial distribution of (a) R and (b) RMSE between observed and estimated $PM_{2.5}$ over the stations.

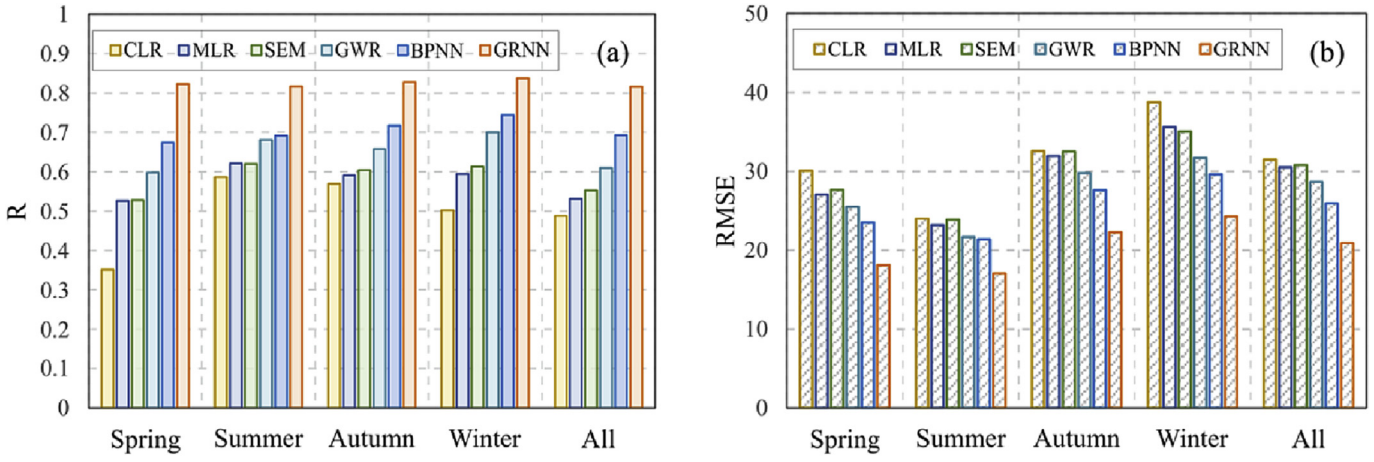


**Fig. 5.** Seasonal variation of (a) R and (b) RMSE between observed and estimated $PM_{2.5}$.

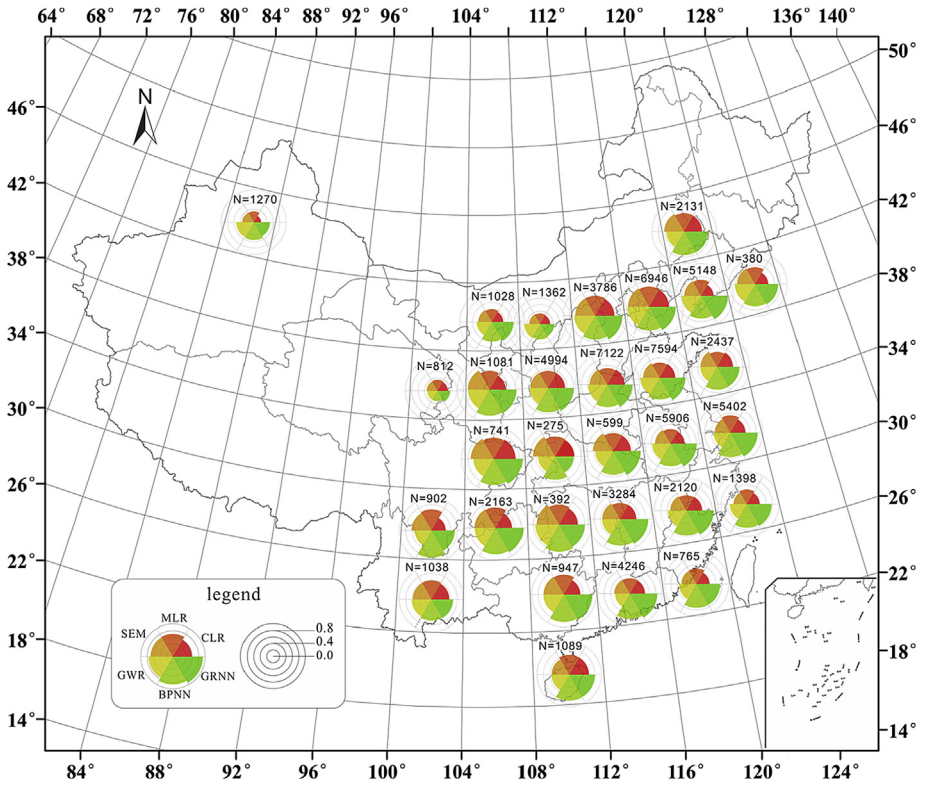


**Fig. 6.** Geographical variation of R values between observed and estimated $PM_{2.5}$ in each 4° × 4° grid box.

(2009b). All the data measured at the stations falling in each grid box were collected. However, some grid boxes containing only a few (<4) stations were eliminated. Fig. 6 shows the geographical variation of R values between observed and estimated $PM_{2.5}$ for the cross-validation, and the summary of the R and RMSE statistics over all the grid boxes is presented in Table 2.

Compared with the performance of the various models at national scale, a similar trend can be seen in most of the grid boxes. That is, the GRNN model performs the best, followed by BPNN and GWR, and CLR gives the poorest performance. However, the GWR model does not report great advantages over the conventional models, and the CLR model obtains almost the same performance as MLR. Additionally, some spatial differences are found. The GRNN model tends to obtain poorer results over the grid boxes in West China. This may be caused by the relatively sparse distribution of the $PM_{2.5}$ monitoring stations in this area. The models, especially the neural network models (BPNN and GRNN), achieve the highest accuracies and stability of performance over those grid boxes which locate between longitudes 112° and 120° and contain more data records. These findings indicate that with more comprehensive data, the neural network models can perform better accordingly.

As Table 2 shows, the R value of the GRNN model ranges from 0.39 to 0.89, with a mean value of 0.75. There is a large decrease (0.82–0.75) from the national R value to the mean R value of the geographical grid boxes for the cross-validation. However, an opposite trend appears for the BPNN. On the other hand, the GRNN model obtains the highest standard deviation (SD = 0.13) of R, meaning the biggest spatial variation of model performance. Meanwhile, the GWR model reports the smallest standard deviation (SD = 0.08) of R, indicating that it is less sensitive to spatial location.

### 4.2. Mapping the mean distribution of $PM_{2.5}$ concentration

In Fig. 7, the yearly mean distributions of $PM_{2.5}$ in China are mapped. The interpolated map presents a relatively coarse distribution of ground-level $PM_{2.5}$ concentrations, although it does not have much detailed spatial information, but it can be considered as a reference. The direct averaging of the GRNN-estimated $PM_{2.5}$ concentration does not share a similar spatial distribution to the interpolated map, with the most obvious difference being that Guangxi province has almost the same level of $PM_{2.5}$ as the BTH region. The results based on the proposed merging strategy share a similar spatial pattern to the interpolated map, but with many more details. Overall, the results suggest that the proposed pixel-based merging strategy is more effective for mapping the

**Table 2**
Summary of the R and RMSE statistics over all the grid boxes.

| | R | | | | | | RMSE | | | | | |
|---|---|---|---|---|---|---|---|---|---|---|---|---|
| | CLR | MLR | SEM | GWR | BPNN | GRNN | CLR | MLR | SEM | GWR | BPNN | GRNN |
| Minimum | 0.22 | 0.33 | 0.34 | 0.32 | 0.32 | 0.39 | 14.87 | 14.58 | 14.75 | 13.49 | 11.64 | 12.30 |
| Maximum | 0.68 | 0.66 | 0.71 | 0.74 | 0.85 | 0.89 | 37.55 | 36.73 | 37.51 | 35.77 | 31.31 | 35.34 |
| Mean | 0.48 | 0.52 | 0.55 | 0.57 | 0.72 | 0.75 | 27.41 | 26.54 | 26.53 | 25.46 | 21.37 | 20.26 |
| SD | 0.10 | 0.10 | 0.11 | 0.08 | 0.11 | 0.13 | 5.34 | 5.61 | 5.43 | 5.49 | 4.72 | 4.76 |

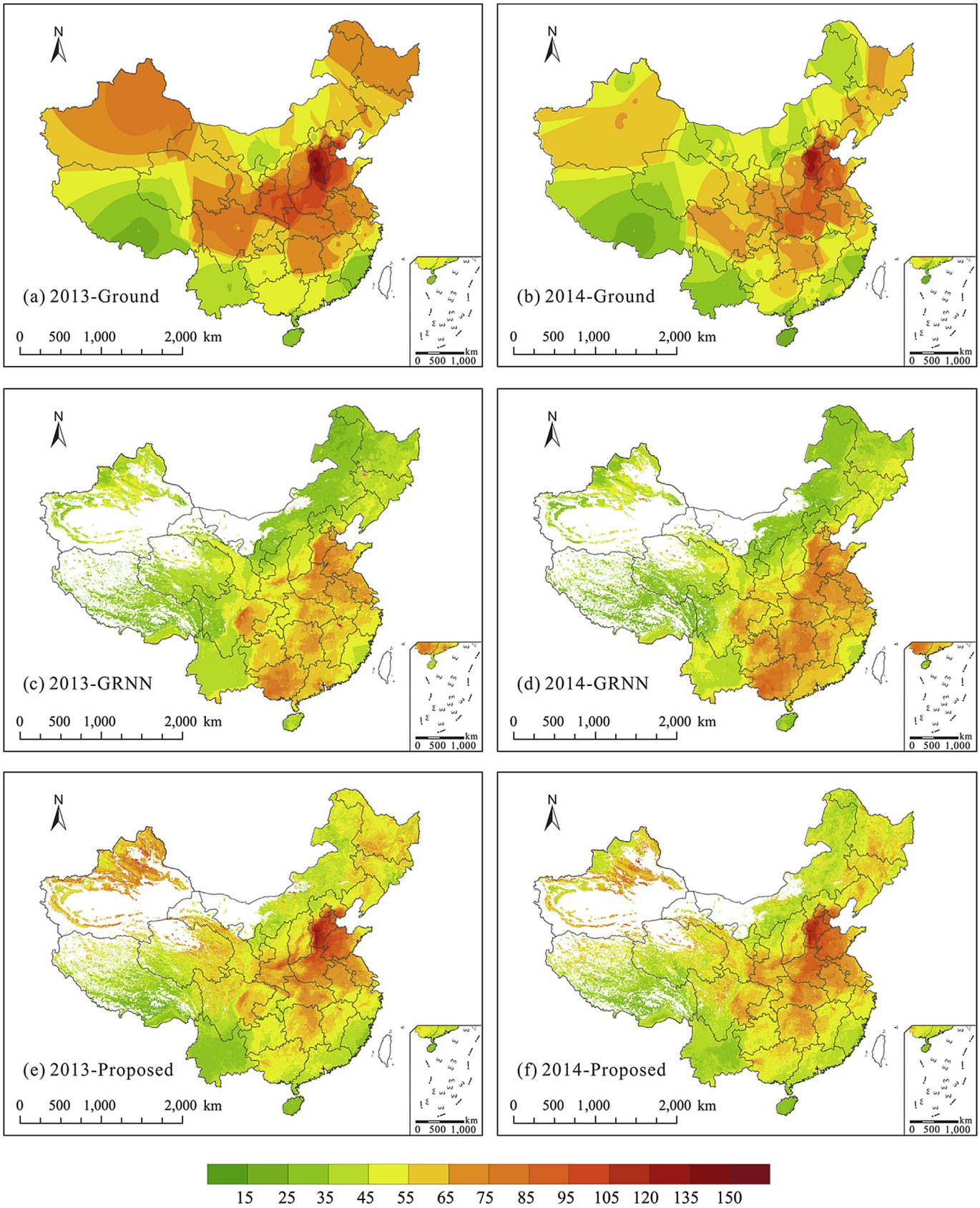


**Fig. 7.** Annual mean distribution of $PM_{2.5}$ concentration ($\mu g/m^3$) in China. Top row: the results interpolated by ground station measurements. Middle row: the direct averaging of GRNN-estimated $PM_{2.5}$ concentration. Bottom row: the mean distribution based on the proposed pixel-based merging strategy. White areas indicate missing data.

distribution of $PM_{2.5}$ in China.

Spatially, the $PM_{2.5}$ pollution in West China is not as serious as that in East China, which is in accordance with the distribution of economic development and urbanization. Moreover, a strong north-to-south decreasing gradient is found, which agrees with the findings of previous studies (Lin et al., 2015). It should be noted that inner China generally suffers from a heavier $PM_{2.5}$ pollution level than the southeastern coast; for instance, Central China (Hunan, Hubei, and Henan provinces) has a higher level of $PM_{2.5}$ concentration than Guangdong and Fujian provinces. In particular, a highly polluted region is located in the North China Plain, with a yearly average $PM_{2.5}$ concentration of about $85–120 \mu g/m^3$. Previous studies (Quan et al., 2011; Tao et al., 2012) showed that rapid industrialization and urbanization have led to serious $PM_{2.5}$ pollution in this area. The cleanest regions are Hainan province, part of Yunnan province, and Tibet, with yearly mean $PM_{2.5}$ concentrations of less than $35 \mu g/m^3$.

The seasonal mean distribution of $PM_{2.5}$ concentration in China was also mapped using the proposed merging strategy. The seasonal maps for 2014 are shown in Fig. 8, where it can be seen that winter is the most polluted season, whereas summer is the cleanest. According to previous studies (Han et al., 2010; Yu et al., 2011), this may be caused by winter heating in North China, Northeast China, and Northwest China.

The distribution of $PM_{2.5}$ concentration is qualitatively similar to the station measurements. To make a further evaluation of the results, the R and RMSE values between the yearly and seasonal mean mapped $PM_{2.5}$ and in situ $PM_{2.5}$ were calculated, respectively. As Table 3 shows, the proposed merging strategy obtains better results than BCM at yearly and seasonal scale, with the R values all greater than 0.90, suggesting that the mapped $PM_{2.5}$ distribution quantitatively agrees quite well with the station measurements.

### 4.3. Discussion

To date, there are two strategies that have been used for point-surface fusion for the estimation of ground-level $PM_{2.5}$ concentration. One strategy is that the models focus on the overall effects on $PM_{2.5}$ concentrations during the whole study period (Gupta and Christopher, 2009a; Lin et al., 2015; Wu et al., 2012); the other

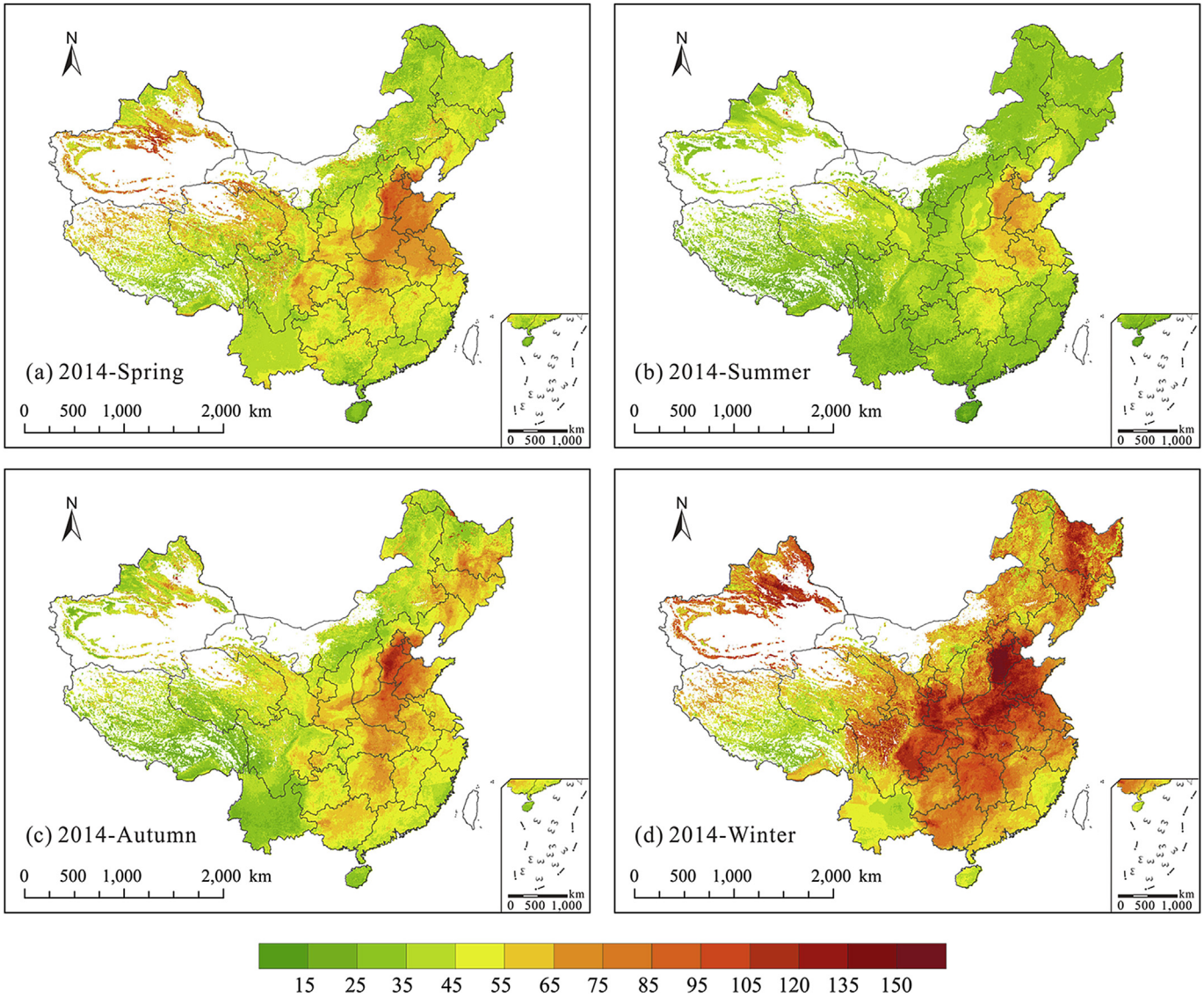


**Fig. 8.** Seasonal mean distribution of $PM_{2.5}$ ($\mu g/m^3$) in China. White areas indicate missing data.

**Table 3**
R and RMSE values between yearly and seasonal mean mapped $PM_{2.5}$ and in situ $PM_{2.5}$.

| Method | | 2013 | | | | | 2014 | | | | |
|---|---|---|---|---|---|---|---|---|---|---|---|
| | | All | Spring | Summer | Autumn | Winter | All | Spring | Summer | Autumn | Winter |
| Proposed | R | 0.96 | 0.93 | 0.95 | 0.94 | 0.96 | 0.95 | 0.93 | 0.93 | 0.92 | 0.95 |
| | RMSE | 6.73 | 7.55 | 6.44 | 9.07 | 13.85 | 6.93 | 7.31 | 6.30 | 8.94 | 10.05 |
| BCM | R | 0.93 | 0.90 | 0.93 | 0.87 | 0.84 | 0.92 | 0.91 | 0.88 | 0.84 | 0.81 |
| | RMSE | 8.56 | 8.72 | 8.07 | 12.72 | 25.62 | 8.18 | 8.04 | 7.76 | 13.08 | 21.80 |

strategy emphasizes a daily basis (Ma et al., 2014, 2016; Song et al., 2014). Clearly, our study can be classified as the former strategy. This strategy can predict the historical $PM_{2.5}$ concentrations which cannot be provided by ground station measurements, whereas the latter strategy has an advantage in the real-time monitoring of $PM_{2.5}$ pollution. To further validate the results obtained in our study, they were compared with the results of one of the former studies (Lin et al., 2015) which focused on a national scale. To some degree, the model performance of the two strategies cannot really be intercompared because of the great differences, but we still made an attempt to qualitatively compare our results with those of the latter studies (Ma et al., 2014, 2016).

A good correlation ($R = 0.90$) between annual mean observed and estimated $PM_{2.5}$ in 2013 was reported in a previous study (Lin et al., 2015). Our results show a slight advantage in $PM_{2.5}$ estimation, with R values between the GRNN-estimated $PM_{2.5}$ and the corresponding observed $PM_{2.5}$ of 0.93 during the same period. On the other hand, we also attempted to compare our results with those based on a daily basis and a grid technique (Ma et al., 2014, 2016). The R and RMSE values of these results are 0.80/0.89 and 32.98/27.42$\mu g/m^3$, whereas we report 0.82 and 20.93$\mu g/m^3$, respectively. There is a decrease in R value from the latter study to ours. However it should be noted that their study and ours have many significant differences in data and methods; for example, AOD gap filling was undertaken in their study. Hence, the variation of R/RMSE cannot be the whole story. Compared with the former study, our results share a similar spatial distribution. However, a slightly higher level of $PM_{2.5}$ concentration in the BTH region and a lower level in the Sichuan Basin are reported. Furthermore, our spatial pattern is also very like their results of the 10-year (2004–2013) $PM_{2.5}$ mean distribution. The North China Plain has the highest level of $PM_{2.5}$ concentration, and a gradual decrease appears from the north to the south.

There are still some limitations to the approach used in this study. On one hand, the newly released 3-km AOD products can better resolve aerosol gradients and retrieve closer to clouds, but they are still susceptible to cloud contamination. Therefore, there may be some potential bias in the 3-km AOD products. However, it should be noted that the 3-km products still perform acceptably against the ground measurements (Munchak et al., 2013). On the other hand, the proposed merging strategy treats the lost data using a statistical method, for both thick and thin clouds/haze. This potential bias could be further analyzed for time and location (Christopher and Gupta, 2010). Using satellite-derived cloud fraction (CF) and cloud optical thickness (COT) to fill the data gaps (Yu et al., 2015) remains one of our future aims.

In addition, the daily average $PM_{2.5}$ data are used to establish the AOD-$PM_{2.5}$ relationship, which ignores the diurnal variability of $PM_{2.5}$ (Guo et al., 2016a; Li et al., 2015a). To evaluate the influence of the diurnal variability of $PM_{2.5}$ on the AOD-$PM_{2.5}$ relationship, hourly $PM_{2.5}$ data should be adopted. However, one of our purposes is to map the yearly and seasonal mean distributions of $PM_{2.5}$ and the hourly data can only represent the $PM_{2.5}$ distribution at certain hours. These data will be used for the real-time monitoring of $PM_{2.5}$, to characterize the diurnal variability of $PM_{2.5}$ in future studies. On the MERRA-2 reanalysis data side, more discussion with regard of the meteorological variables, especially the planetary boundary layer height (HPBL), should be considered. HPBL is one of the dominant parameters influencing the AOD-$PM_{2.5}$ relationship, which has large uncertainties across China (Guo et al., 2016b). Incorporating the sounding-based HPBL data into the GRNN model appears to be a promising method to better estimate ground-level $PM_{2.5}$ concentration.

## 5. Conclusions

To sum up, our study has several benefits and advantages compared with the previous studies. Firstly, we have applied the new GRNN model to better describe the AOD-$PM_{2.5}$ relationship. Secondly, the performance of various widely used models has been evaluated and compared at national scale. Finally, a pixel-based merging strategy has been proposed to effectively map the yearly and seasonal mean distribution of $PM_{2.5}$ concentration in China.

With cross-validated R values of 0.49–0.55 and RMSEs of 30.80–31.51$\mu g/m^3$, the conventional models did not perform as well at national scale as they did at regional scale. In contrast, the more advanced models achieved better performances in $PM_{2.5}$ estimation, with R values of 0.61–0.82 and RMSEs of 20.93–28.68$\mu g/m^3$. The proposed GRNN model obtained the best results, with the highest R (0.82) value and lowest RMSE (20.93$\mu g/m^3$) among all the models. The R values between the yearly/seasonal mean mapped $PM_{2.5}$ and observed $PM_{2.5}$ were all greater than 0.90, indicating that the mapped $PM_{2.5}$ distribution agrees quite well with the station measurements. This approach therefore has the capacity to provide reasonable information for the spatiotemporal analysis of $PM_{2.5}$ variation.

In future studies, we will focus on three aspects. Firstly, statistical methods will be introduced into filling the missing AOD data (Li et al., 2015b; Shen et al., 2015; Zeng et al., 2013), because a wider coverage of satellite-based AOD could provide more comprehensive information for $PM_{2.5}$ estimation. Secondly, we will take more variables into consideration; for example, land use and population. A sensitivity analysis will also be conducted to select parameters more closely associated with $PM_{2.5}$ pollution, to improve the estimation accuracy. Finally, a long-term analysis of $PM_{2.5}$ pollution in China will be made to facilitate epidemiological studies about the impact of air pollution on public health, using the estimated $PM_{2.5}$ concentration at a 3-km resolution.

## Acknowledgments

This work was supported by the National Key Research and Development Program of China (2016YFC0200900) and the National Natural Science Foundation of China (41422108 and 41271376). We would also like to thank the data providers of the China National Environmental Monitoring Center (CNEMC), the Goddard Space Flight Center Distributed Active Archive Center (GSFC DAAC), and the US National Aeronautics and Space Administration (NASA) Data Center.

## References


Bartell, S.M., Longhurst, J., Tjoa, T., Sioutas, C., Delfino, R.J., 2013. Particulate air pollution, ambulatory heart rate variability, and cardiac arrhythmia in retirement community residents with coronary artery disease. Environ. Health Perspect. 121, 1135–1141.

Beloconi, A., Kamarianakis, Y., Chrysoulakis, N., 2016. Estimating urban $PM_{10}$ and $PM_{2.5}$ concentrations, based on synergistic MERIS/AATSR aerosol observations, land cover and morphology data. Remote Sens. Environ. 172, 148–164.

Benas, N., Beloconi, A., Chrysoulakis, N., 2013. Estimation of urban $PM_{10}$ concentration, based on MODIS and MERIS/AATSR synergistic observations. Atmos. Environ. 79, 448–454.

Christopher, S.A., Gupta, P., 2010. Satellite remote sensing of particulate matter air quality: the cloud-cover problem. J. Air Waste Manage. Assoc. 60, 596–602.

Chu, D.A., Kaufman, Y.J., Zibordi, G., Chern, J.D., Mao, J., Li, C., Holben, B.N., 2003. Global monitoring of air pollution over land from the Earth observing system-terra moderate resolution imaging spectroradiometer (MODIS). J. Geophys. Res. Atmos. 108.

Cigizoglu, H.K., Alp, M., 2006. Generalized regression neural network in modelling river sediment yield. Adv. Eng. Softw. 37, 63–68.

De Leeuw, J., Jia, H., Yang, L., Liu, X., Schmidt, K., Skidmore, A.K., 2006. Comparing accuracy assessments to infer superiority of image classification methods. Int. J. Remote Sens. 27, 223–232.

Engel-Cox, J., Kim Oanh, N.T., van Donkelaar, A., Martin, R.V., Zell, E., 2013. Toward the next generation of air quality monitoring: particulate Matter. Atmos. Environ. 80, 584–590.

Fang, X., Zou, B., Liu, X., Sternberg, T., Zhai, L., 2016. Satellite-based ground $PM_{2.5}$ estimation using timely structure adaptive modeling. Remote Sens. Environ. 186, 152–163.

Gardner, M.W., Dorling, S.R., 1998. Artificial neural networks (the multilayer perceptron)—a review of applications in the atmospheric sciences. Atmos. Environ. 32, 2627–2636.

Geng, G., Zhang, Q., Martin, R.V., van Donkelaar, A., Huo, H., Che, H., Lin, J., He, K., 2015. Estimating long-term $PM_{2.5}$ concentrations in China using satellite-based aerosol optical depth and a chemical transport model. Remote Sens. Environ. 166, 262–270.

Guo, J., Deng, M., Lee, S.S., Wang, F., Li, Z., Zhai, P., Liu, H., Lv, W., Yao, W., Li, X., 2016a. Delaying precipitation and lightning by air pollution over the Pearl River Delta. Part I: observational analyses. J. Geophys. Res. Atmos. 121, 6472–6488.

Guo, J., Miao, Y., Zhang, Y., Liu, H., Li, Z., Zhang, W., He, J., Lou, M., Yan, Y., Bian, L., Zhai, P., 2016b. The climatology of planetary boundary layer height in China derived from radiosonde and reanalysis data. Atmos. Chem. Phys. 16, 13309–13319.

Guo, J., Zhang, X., Che, H., Gong, S., An, X., Cao, C., Jie, G., Zhang, H., Wang, Y., Zhang, X., 2009. Correlation between PM concentrations and aerosol optical depth in eastern China. Atmos. Environ. 43, 5876–5886.

Gupta, P., Christopher, S.A., 2009a. Particulate matter air quality assessment using integrated surface, satellite, and meteorological products: 2. A neural network approach. J. Geophys. Res. Atmos. 114, D20205.

Gupta, P., Christopher, S.A., 2009b. Particulate matter air quality assessment using integrated surface, satellite, and meteorological products: multiple regression approach. J. Geophys. Res. Atmos. 114, D14205.

Han, B., Kong, S., Bai, Z., Du, G., Bi, T., Li, X., Shi, G., Hu, Y., 2010. Characterization of elemental species in $PM_{2.5}$ samples collected in four cities of Northeast China. Water Air Soil Pollut. 209, 15–28.

Hoff, R.M., Christopher, S.A., 2009. Remote sensing of particulate pollution from space: have we reached the promised land? J. Air Waste Manage. Assoc. 59, 645–675.

Hu, X., Waller, L.A., Al-Hamdan, M.Z., Crosson, W.L., Estes Jr., M.G., Estes, S.M., Quattrochi, D.A., Sarnat, J.A., Liu, Y., 2013. Estimating ground-level $PM_{2.5}$ concentrations in the southeastern U.S. using geographically weighted regression. Environ. Res. 121, 1–10.

Hu, X., Waller, L.A., Lyapustin, A., Wang, Y., Al-Hamdan, M.Z., Crosson, W.L., Estes Jr., M.G., Estes, S.M., Quattrochi, D.A., Puttaswamy, S.J., Liu, Y., 2014a. Estimating ground-level $PM_{2.5}$ concentrations in the Southeastern United States using MAIAC AOD retrievals and a two-stage model. Remote Sens. Environ. 140, 220–232.

Hu, X., Waller, L.A., Lyapustin, A., Wang, Y., Liu, Y., 2014b. 10-year spatial and temporal trends of $PM_{2.5}$ concentrations in the southeastern US estimated using high-resolution satellite data. Atmos. Chem. Phys. 14, 6301–6314.

Kloog, I., Chudnovsky, A.A., Just, A.C., Nordio, F., Koutrakis, P., Coull, B.A., Lyapustin, A., Wang, Y., Schwartz, J., 2014. A new hybrid spatio-temporal model for estimating daily multi-year $PM_{2.5}$ concentrations across northeastern USA using high resolution aerosol optical depth data. Atmos. Environ. 95, 581–590.

Kloog, I., Koutrakis, P., Coull, B.A., Lee, H.J., Schwartz, J., 2011. Assessing temporally and spatially resolved $PM_{2.5}$ exposures for epidemiological studies using satellite aerosol optical depth measurements. Atmos. Environ. 45, 6267–6275.

Li, C., Hsu, N.C., Tsay, S.-C., 2011. A study on the potential applications of satellite data in air quality monitoring and forecasting. Atmos. Environ. 45, 3663–3675.

Li, C., Mao, J., Lau, A.K.H., Yuan, Z., Wang, M., Liu, X., 2005. Application of MODIS satellite products to the air pollution research in Beijing. Sci. China Earch Sci. 48, 209–219.

Li, R., Li, Z., Gao, W., Ding, W., Xu, Q., Song, X., 2015a. Diurnal, seasonal, and spatial variation of $PM_{2.5}$ in Beijing. Sci. Bull. 60, 387–395.

Li, X., Shen, H., Zhang, L., Li, H., 2015b. Sparse-based reconstruction of missing information in remote sensing images from spectral/temporal complementary information. ISPRS J. Photogramm. 106, 1–15.

Li, Z., Zhang, Y., Shao, J., Li, B., Hong, J., Liu, D., Li, D., Wei, P., Li, W., Li, L., Zhang, F., Guo, J., Deng, Q., Wang, B., Cui, C., Zhang, W., Wang, Z., Lv, Y., Xu, H., Chen, X., Li, L., Qie, L., 2016. Remote sensing of atmospheric particulate mass of dry $PM_{2.5}$ near the ground: method validation using ground-based measurements. Remote Sens. Environ. 173, 59–68.

Lin, C., Li, Y., Yuan, Z., Lau, A.K.H., Li, C., Fung, J.C.H., 2015. Using satellite remote sensing data to estimate the high-resolution distribution of ground-level $PM_{2.5}$. Remote Sens. Environ. 156, 117–128.

Liu, Y., Franklin, M., Kahn, R., Koutrakis, P., 2007. Using aerosol optical thickness to predict ground-level $PM_{2.5}$ concentrations in the St. Louis area: a comparison between MISR and MODIS. Remote Sens. Environ. 107, 33–44.

Liu, Y., Park, R.J., Jacob, D.J., Li, Q., Kilaru, V., Sarnat, J.A., 2004. Mapping annual mean ground-level $PM_{2.5}$ concentrations using Multiangle Imaging Spectroradiometer aerosol optical thickness over the contiguous United States. J. Geophys. Res. Atmos. 109, D22206.

Liu, Y., Sarnat, J.A., Kilaru, V., Jacob, D.J., Koutrakis, P., 2005. Estimating ground-level PM2.5 in the eastern United States using satellite remote sensing. Environ. Sci. Technol. 39, 3269–3278.

Liu, Y., Schichtel, B.A., Koutrakis, P., 2009. Estimating particle sulfate concentrations using MISR retrieved aerosol properties. IEEE J. Sel. Top. Appl. Earth Observ. Remote Sens 2, 176–184.

Ma, Z., Hu, X., Huang, L., Bi, J., Liu, Y., 2014. Estimating ground-level $PM_{2.5}$ in China using satellite remote sensing. Environ. Sci. Technol. 48, 7436–7444.

Ma, Z., Hu, X., Sayer, A.M., Levy, R., Zhang, Q., Xue, Y., Tong, S., Bi, J., Huang, L., Liu, Y., 2016. Satellite-based spatiotemporal trends in $PM_{2.5}$ concentrations: China, 2004-2013. Environ. Health Perspect. 124, 184–192.

Martin, R.V., 2008. Satellite remote sensing of surface air quality. Atmos. Environ. 42, 7823–7843.

Molod, A., Takacs, L., Suarez, M., Bacmeister, J., 2015. Development of the GEOS-5 atmospheric general circulation model: evolution from MERRA to MERRA2. Geosci. Model Dev. 8, 1339–1356.

Munchak, L.A., Levy, R.C., Mattoo, S., Remer, L.A., Holben, B.N., Schafer, J.S., Hostetler, C.A., Ferrare, R.A., 2013. MODIS 3 km aerosol product: applications over land in an urban/suburban region. Atmos. Meas. Tech. 6, 1747–1759.

Ordieres, J.B., Vergara, E.P., Capuz, R.S., Salazar, R.E., 2005. Neural network prediction model for fine particulate matter ($PM_{2.5}$) on the US–Mexico border in El Paso (Texas) and Ciudad Juárez (Chihuahua). Environ. Modell. Softw. 20, 547–559.

Peng, J., Chen, S., Lü, H., Liu, Y., Wu, J., 2016. Spatiotemporal patterns of remotely sensed $PM_{2.5}$ concentration in China from 1999 to 2011. Remote Sens. Environ. 174, 109–121.

Quan, J., Zhang, Q., He, H., Liu, J., Huang, M., Jin, H., 2011. Analysis of the formation of fog and haze in North China Plain (NCP). Atmos. Chem. Phys. 11, 8205–8214.

Reich, S.L., Gomez, D.R., Dawidowski, L.E., 1999. Artificial neural network for the identification of unknown air pollution sources. Atmos. Environ. 33, 3045–3052.

Remer, L.A., Kaufman, Y.J., Tanré, D., Mattoo, S., Chu, D.A., Martins, J.V., Li, R.R., Ichoku, C., Levy, R.C., Kleidman, R.G., Eck, T.F., Vermote, E., Holben, B.N., 2005. The MODIS aerosol algorithm, products, and validation. J. Atmos. Sci. 62, 947–973.

Rodriguez, J.D., Perez, A., Lozano, J.A., 2010. Sensitivity analysis of k-Fold Cross validation in prediction error estimation. IEEE Trans. Pattern Anal. Mach. Intell. 32, 569–575.

Sacks, J.D., Stanek, L.W., Luben, T.J., Johns, D.O., Buckley, B.J., Brown, J.S., Ross, M., 2011. Particulate matter-induced health effects: who is susceptible? Environ. Health Perspect. 119, 446–454.

Shen, H., Li, X., Cheng, Q., Zeng, C., Yang, G., Li, H., Zhang, L., 2015. Missing information reconstruction of remote sensing data: a technical review. IEEE Geosci. Remote Sens. Mag. 3, 61–85.

Shen, H., Wu, P., Liu, Y., Ai, T., Wang, Y., Liu, X., 2013. A spatial and temporal reflectance fusion model considering sensor observation differences. Int. J. Remote Sens. 34, 4367–4383.

Song, W., Jia, H., Huang, J., Zhang, Y., 2014. A satellite-based geographically weighted regression model for regional $PM_{2.5}$ estimation over the Pearl River Delta region in China. Remote Sens. Environ. 154, 1–7.

Specht, D.F., 1991. A general regression neural network. IEEE Trans. Neural. Netw. 2, 568–576.

Specht, D.F., 1993. The general regression neural network—Rediscovered. Neural Netw. 6, 1033–1034.

Tao, M., Chen, L., Su, L., Tao, J., 2012. Satellite observation of regional haze pollution over the North China Plain. J. Geophys. Res. Atmos. 117.

Tian, J., Chen, D., 2010. A semi-empirical model for predicting hourly ground-level fine particulate matter ($PM_{2.5}$) concentration in southern Ontario from satellite remote sensing and ground-based meteorological measurements. Remote Sens. Environ. 114, 221–229.

van Donkelaar, A., Martin, R.V., Brauer, M., Kahn, R., Levy, R., Verduzco, C., Villeneuve, P.J., 2010. Global estimates of ambient fine particulate matter concentrations from satellite-based aerosol optical depth: development and application. Environ. Health Perspect. 118, 847–855.

van Donkelaar, A., Martin, R.V., Pasch, A.N., Szykman, J.J., Zhang, L., Wang, Y.X., Chen, D., 2012. Improving the accuracy of daily satellite-derived ground-level fine aerosol concentration estimates for north America. Environ. Sci. Technol.

46, 11971–11978.
Wang, Z., Chen, L., Tao, J., Zhang, Y., Su, L., 2010. Satellite-based estimation of regional particulate matter (PM) in Beijing using vertical-and-RH correcting method. Remote Sens. Environ. 114, 50–63.
Wu, P., Shen, H., Ai, T., Liu, Y., 2013. Land-surface temperature retrieval at high spatial and temporal resolutions based on multi-sensor fusion. Int. J. Digit. Earth 6, 113–133.
Wu, P., Shen, H., Zhang, L., Göttsche, F.-M., 2015. Integrated fusion of multi-scale polar-orbiting and geostationary satellite observations for the mapping of high spatial and temporal resolution land surface temperature. Remote Sens. Environ. 156, 169–181.
Wu, Y., Guo, J., Zhang, X., Tian, X., Zhang, J., Wang, Y., Duan, J., Li, X., 2012. Synergy of satellite and ground based observations in estimation of particulate matter in eastern. China. Sci. Total Environ. 433, 20–30.
Yao, L., Lu, N., 2014. Spatiotemporal distribution and short-term trends of particulate matter concentration over China, 2006–2010. Environ. Sci. Pollut. R. 21, 9665–9675.
You, W., Zang, Z., Zhang, L., Li, Z., Chen, D., Zhang, G., 2015. Estimating ground-level $PM_{10}$ concentration in northwestern China using geographically weighted regression based on satellite AOD combined with CALIPSO and MODIS fire count. Remote Sens. Environ. 168, 276–285.
Yu, C., Di Girolamo, L., Chen, L., Zhang, X., Liu, Y., 2015. Statistical evaluation of the feasibility of satellite-retrieved cloud parameters as indicators of $PM_{2.5}$ levels. J. Expos Sci. Environ. Epidemiol. 25, 457–466.
Yu, X., 1992. Can backpropagation error surface not have local minima. IEEE Trans. Neural. Netw. 3, 1019–1021.
Yu, Y., Schleicher, N., Norra, S., Fricker, M., Dietze, V., Kaminski, U., Cen, K., Stuben, D., 2011. Dynamics and origin of $PM_{2.5}$ during a three-year sampling period in Beijing, China. J. Environ. Monit. 13, 334–346.
Yuan, Y., Liu, S., Castro, R., Pan, X., 2012. $PM_{2.5}$ monitoring and mitigation in the cities of China. Environ. Sci. Technol. 46, 3627–3628.
Zeng, C., Shen, H., Zhang, L., 2013. Recovering missing pixels for Landsat ETM + SLC-off imagery using multi-temporal regression analysis and a regularization method. Remote Sens. Environ. 131, 182–194.
Zhang, Y., Cao, F., 2015. Fine particulate matter ($PM_{2.5}$) in China at a city level. Sci. Rep. 5, 14884.
Zhang, Y., Li, Z., 2015. Remote sensing of atmospheric fine particulate matter ($PM_{2.5}$) mass concentration near the ground from satellite observation. Remote Sens. Environ. 160, 252–262.
Zheng, Y., Zhang, Q., Liu, Y., Geng, G., He, K., 2016. Estimating ground-level PM2.5 concentrations over three megalopolises in China using satellite-derived aerosol optical depth measurements. Atmos. Environ. 124 (Part B), 232–242.